Supplemental Figures and Legends

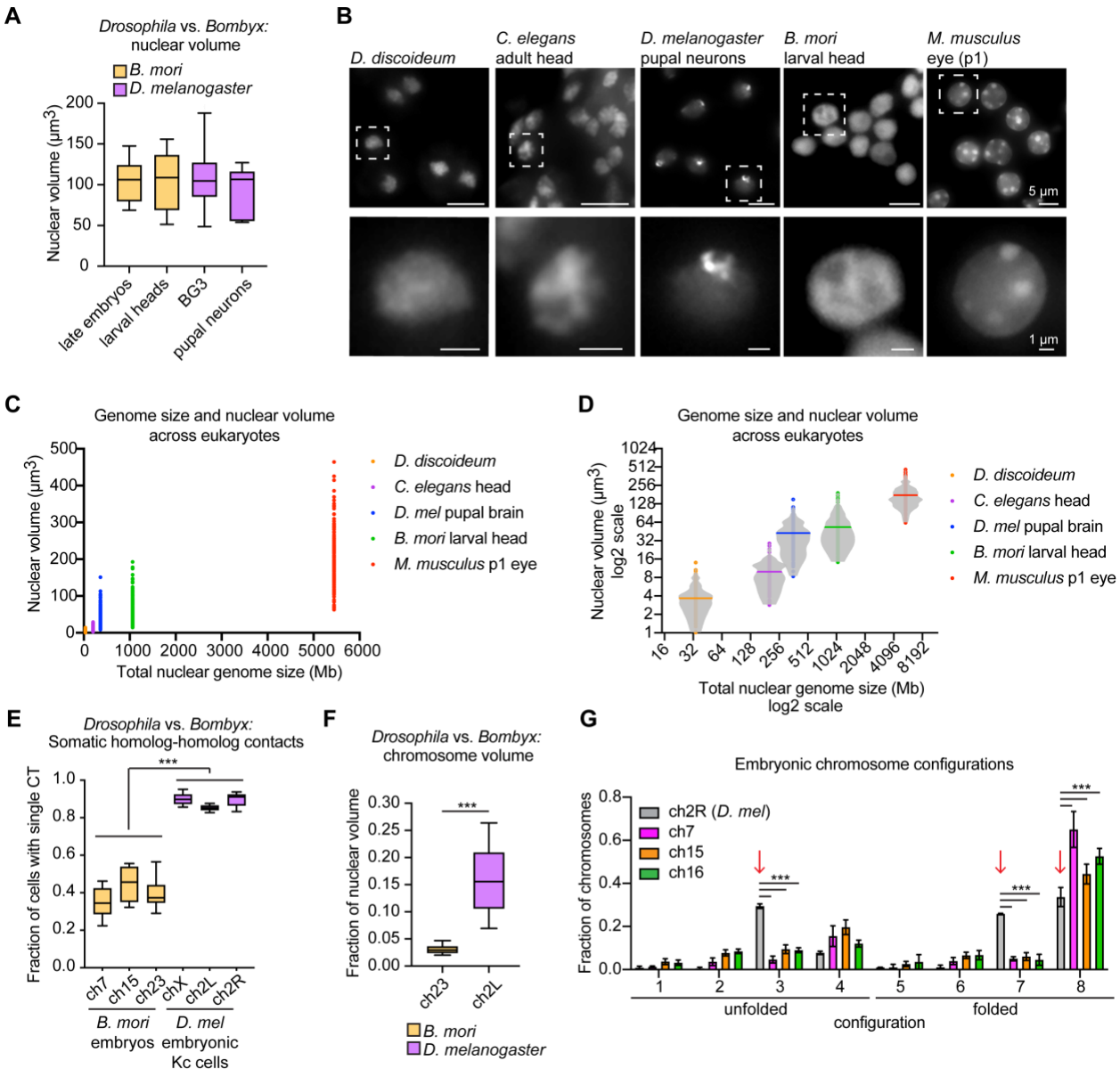

Figure S1. *B. mori* nuclei and chromosomes are relatively more compact than their *D. melanogaster* counterparts.

A) Tukey box and whiskers plot showing the average nuclear volume of *B. mori* diploid cells from late embryos and larval heads (orange) and *D. melanogaster* BG3 cultured cells and pupal neurons (purple). Plots show the averages from 7-15 biological replicates.

B) DAPI stained nuclei. The source species and tissues are indicated above. Dashed squares indicated the zoomed panel below. Species included: *Dictyostelium discoideum* (commonly known as Dicty)*, Caenorhabditis elegans, Drosophila melanogaster (D. mel), Bombyx mori,* and *Mus musculus.*

C-D) Genomic size versus nuclear volume for the species shown in B. In D, each dot represents a single nucleus. Data were gathered from three biological replicates. N= 288 (fly), 317 (mouse), 268 (moth), 209 (worm), 285 (Dicty).

E) Tukey box and whiskers plot showing the average fraction of cells harboring a single contiguous CT for three representative chromosomes in *B. mori* embryos (orange) and 3 representative chromosome arms in *D. melanogaster* embryonic Kc cells (purple). ***p<0.0001; Mann-Whitney Test for all pairwise comparisons.

F) Tukey box and whiskers plot showing the average size (fraction of nuclear volume) for *B. mori* chromosome 23 (orange) from embryonic cells, and *D. melanogaster* ch2L (purple) from BG3 cells. Data shown represent a single biological replicate (n = 1500 cells from *B. mori* and n = 2017 cells from *D. melanogaster*), but similar results were found in 3-5 additional replicates. ***p<0.0001; Mann-Whitney Test.

G) Quantification of folding for *B. mori* embryonic ch7 (magenta), 15 (orange), and 16 (green), and *D. melanogaster* ch2R from embryonic Kc cells (gray). Red arrows indicate configurations enriched in Kc cells (3, 7, 8). Bars show the average of at least three biological replicates with at least 100 cells analyzed from each replicate. Error bars show standard deviation. ***p < 0.0001; Multiple t-tests.

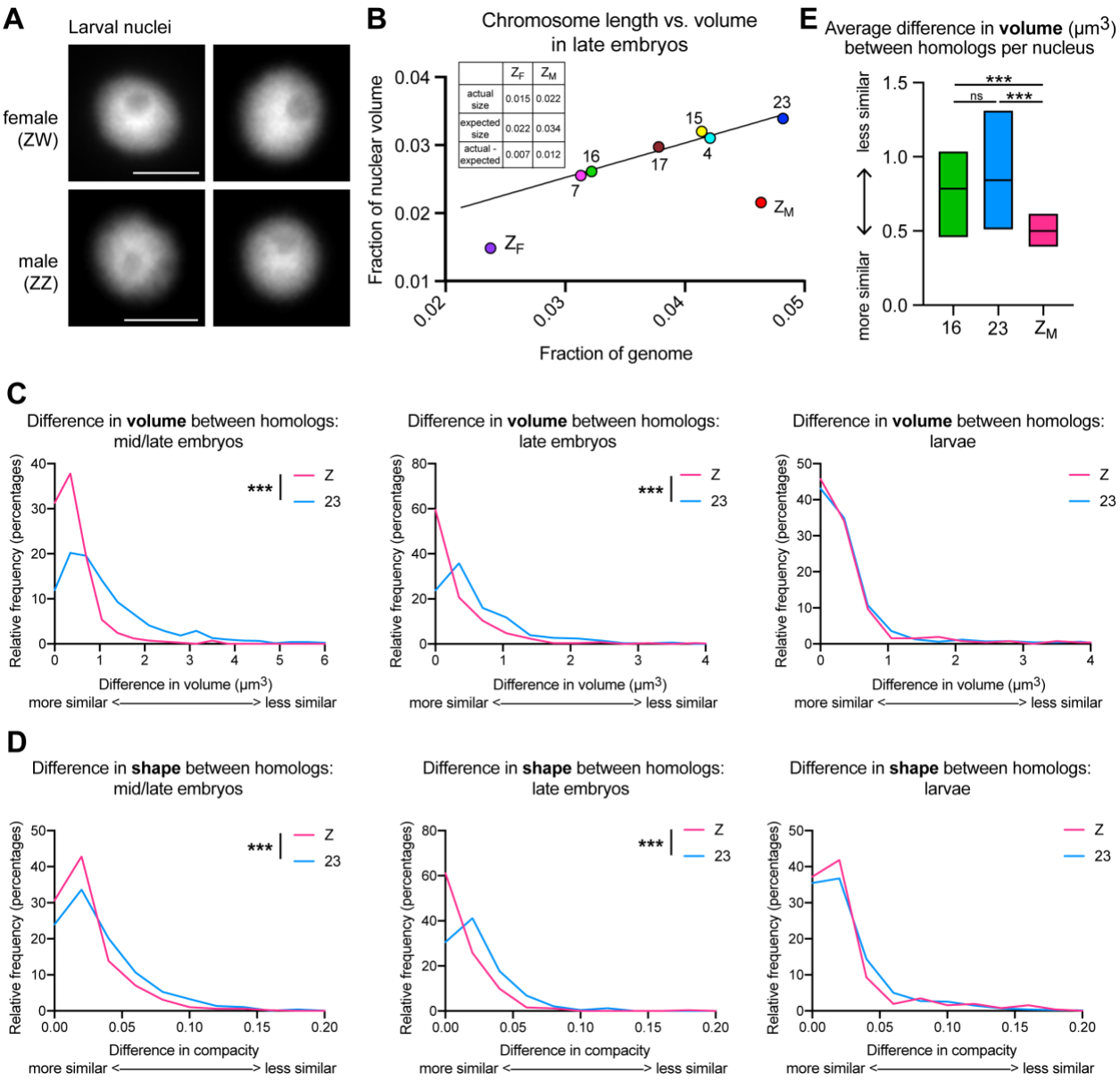

Figure S2. Both male chZ homologs are more similar in size and shape than the ch23 homologs.

A) DAPI staining of representative larval nuclei from B. mori females (top) and males (bottom). Scale bar = 2.5 µm.

B) Dot plot showing chromosome genomic length as a fraction of total genome size (X-axis) versus CT volume as a fraction of nuclear volume (Y-axis). $R^2 = 0.966$ excluding chZ. Data shown are from late embryos.Frequency histograms showing the difference in volume (μm^3) between homologs for chZ (pink) and ch23 (blue) in male mid/late embryos (left),

late embryos (middle), and larvae (right). Data represent a single biological replicate. ***p < 0.0001; Mann-Whitney Test.

C) Frequency histograms showing the difference in shape (compacity) between homologs for chZ (pink) and ch23 (blue) in male mid/late embryos (left), late embryos (middle), and larvae (right). Data represent a single biological replicate. ***p < 0.0001; Mann-Whitney Test.

D) Quantification of interhomolog differences in volume (μm^3) in for ch16 (green), ch23 (blue), and chZ (pink) in male mid/late embryos. Mid-line = mean. Statistics = Mann-Whitney Test. *** p < 0.0001.

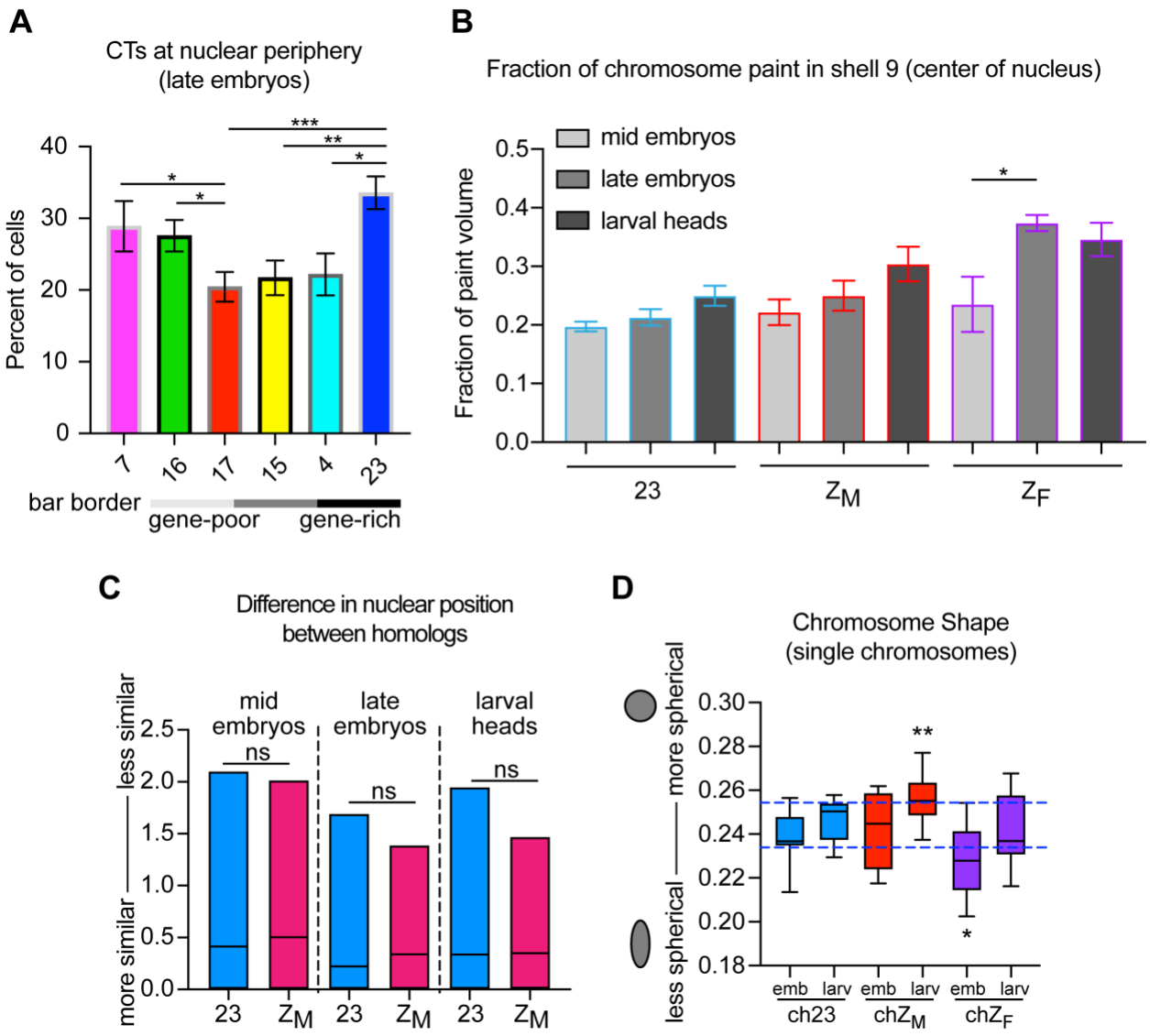

Figure S3. Female chZ is reposition toward the nuclear center and is upregulated in late embryos.

A) Quantification of fraction of autosomes at nuclear periphery in late embryos (defined as having any volume in shells 1-3 of a shell analysis). Bars show average of biological replicates. Error bars show standard error of the mean. Statistics = unpaired t-tests. *p = 0.01 - 0.05, **p = 0.001 - 0.005, ***p < 0.001. Gene density of chromosomes is indicated by bar outlines, with darker outlines indicating higher gene density.

B) Quantification of the fraction of CTs in the nuclear center (defined as having any volume in shell 9 of a shell analysis). Bars show the average between biological replicates. Error bars show standard error of the mean. *p=0.05; unpaired t-test.

C) Quantification of interhomolog differences in nuclear position as measured by the distance from the nuclear edge (μm) for ch23 (blue) or chZ (pink) in male embryos or larvae. Mid-line = mean. Statistics = unpaired t-tests.

D) Tukey box and whisker plot showing quantification of chromosome shape (compacity; Y-axis) for individual chromosomes at the indicated time points. Midline = median. Statistics = Welch's T-tests. *$p < 0.05$, **$p < 0.01$. Blue dashed lines indicate the shape range of ch23.

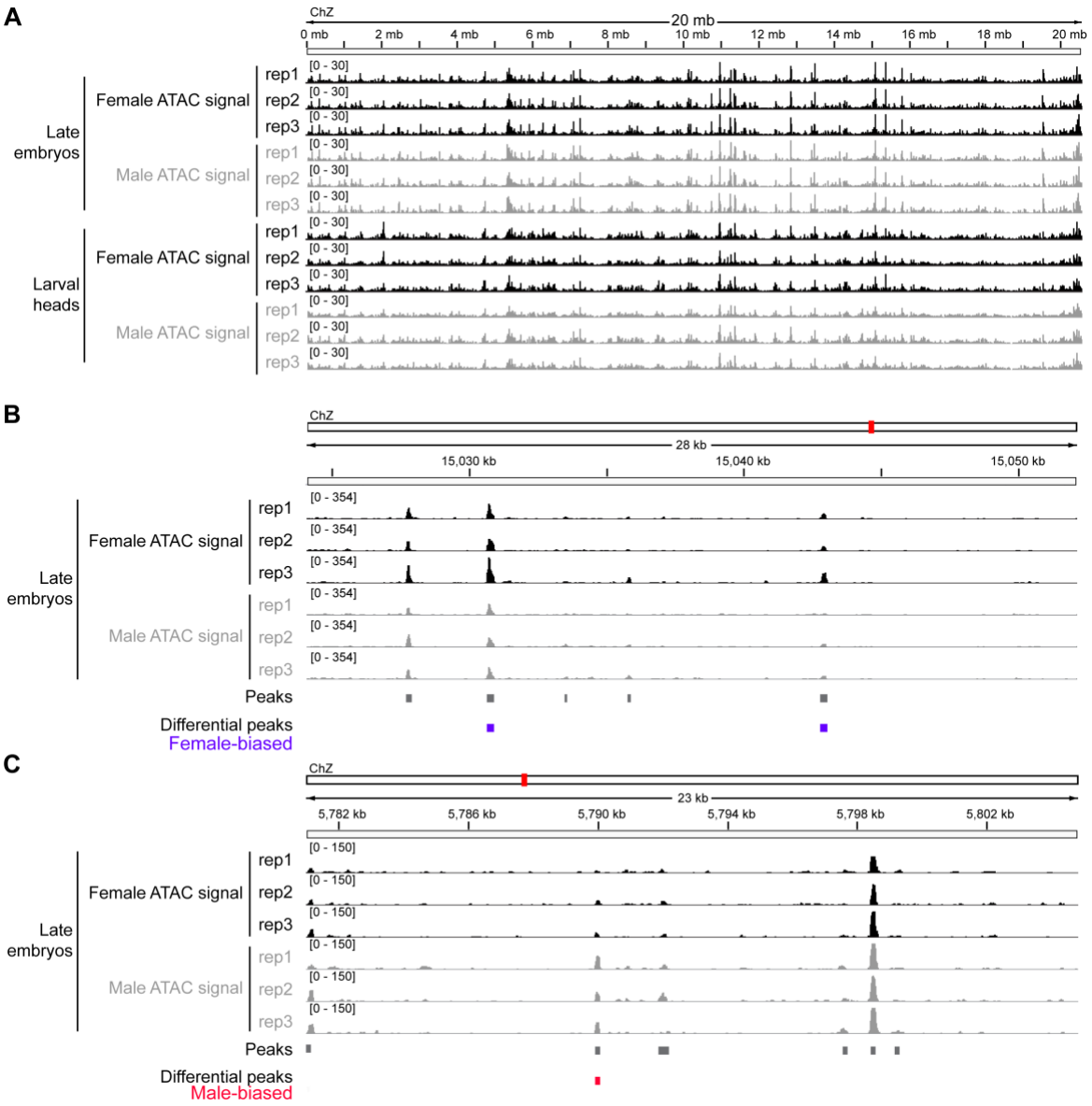

Figure S4. ATAC-seq signal from male and female *B. mori.*

A) ATAC-seq on the entire Z chromosome from male (ZZ) and female (ZW) late embryos (top) and larval heads (bottom). Tracks from three biological replicates are shown. Female tracks are shown in black. Male tracks are shown in gray.

B-C) Zoom of tracks showing a region on chZ (indicated by red box on chromosome schematic, above) with female-biased ATAC-seq (B) or male-biased ATAC-seq (C) in embryos. Peaks called in all replicates are shown in gray/black below the tracks. Female-biased peaks are indicated below in purple. Male-biased peaks are indicated below in red.

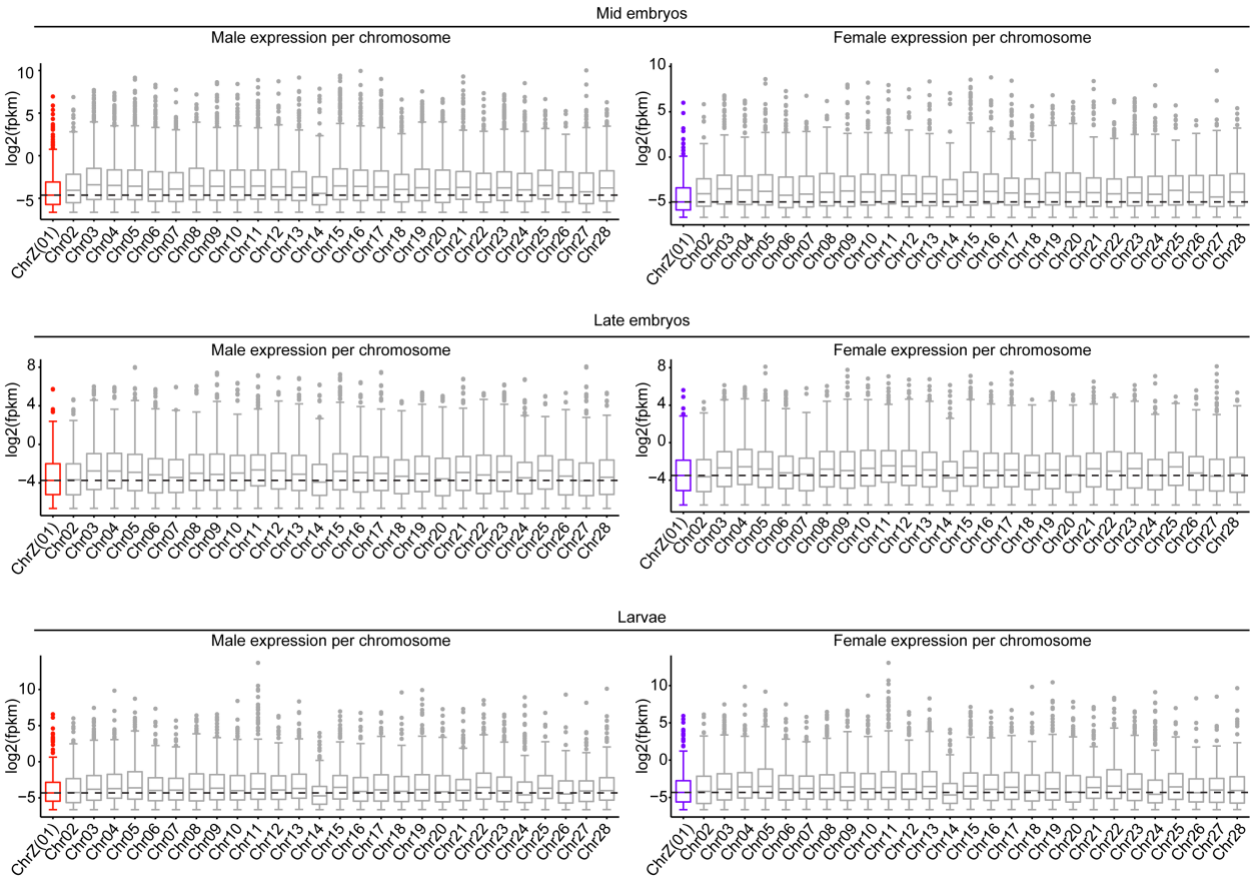

Figure S5. Box plots of expression per chromosome per time point.

Mid-lines represent median values. Black dashed line represents the median of chZ. Each dot represents an expressed gene (fpkm > 0.01). ChZ is shown in red (males) or purple (females). Autosomes are shown in gray.

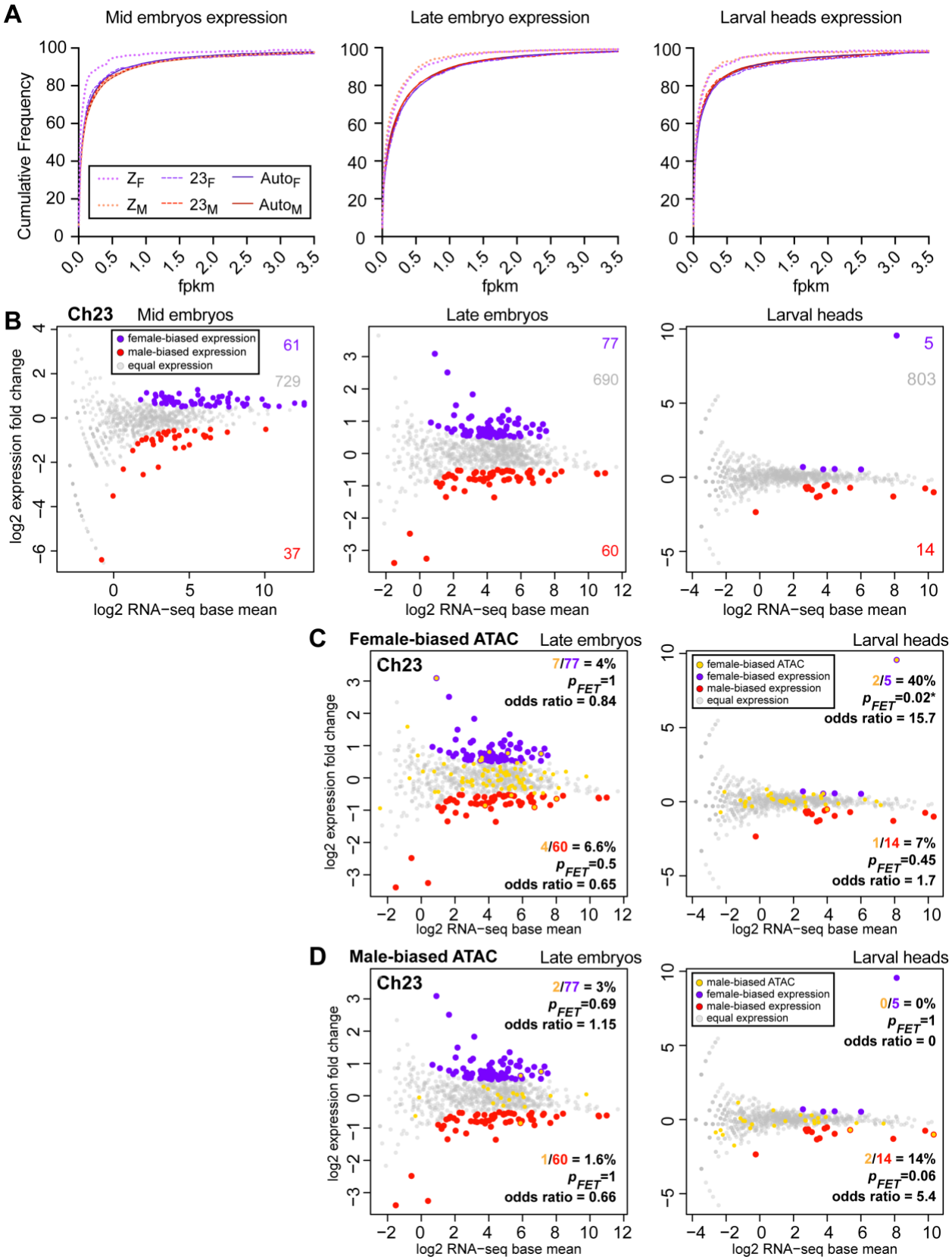
A
Mid embryos expression
Late embryo expression
Larval heads expression
Cumulative Frequency
fpkm
Z_F 23_F $Auto_F$
Z_M 23_M $Auto_M$
B
Ch23
Mid embryos
Late embryos
Larval heads
female-biased expression
male-biased expression
equal expression
61
729
37
77
690
60
5
803
14
log2 expression fold change
log2 RNA−seq base mean
C
Female-biased ATAC
Late embryos
Larval heads
female-biased ATAC
7/77 = 4%
p_{FET}=1
odds ratio = 0.84
4/60 = 6.6%
p_{FET}=0.5
odds ratio = 0.65
2/5 = 40%
p_{FET}=0.02*
odds ratio = 15.7
1/14 = 7%
p_{FET}=0.45
odds ratio = 1.7
D
Male-biased ATAC
male-biased ATAC
2/77 = 3%
p_{FET}=0.69
odds ratio = 1.15
1/60 = 1.6%
p_{FET}=1
odds ratio = 0.66
0/5 = 0%
p_{FET}=1
odds ratio = 0
2/14 = 14%
p_{FET}=0.06
odds ratio = 5.4

Figure S6. RNA-seq on ch23 and all autosomes reveals approximately equal male- and female-biased genes.

A. Cumulative frequency histograms for expression (fpkm) in mid embryos (left), late embryos (middle), and larvae (right).

B. MA plots showing differential expression on ch23 between male and female mid embryos (left), late embryos (middle), and larval heads (left). Loci with significantly differential expression ($q < 0.01$ and fold-change > +/-0.5) are shown in red (male-biased) or purple (female-biased). Numbers of differential or equally expressed loci are indicated to the right.

C-D. MA plots shown in B with genes at or near differential ATAC-seq peaks indicated in Yellow for (C) female-biased ATAC-seq or (D) male-biased ATAC-seq. MA plots for late embryos are on the left, larval heads on the right. Two-sided Fisher's exact test was used to calculate p-values and odds ratios.

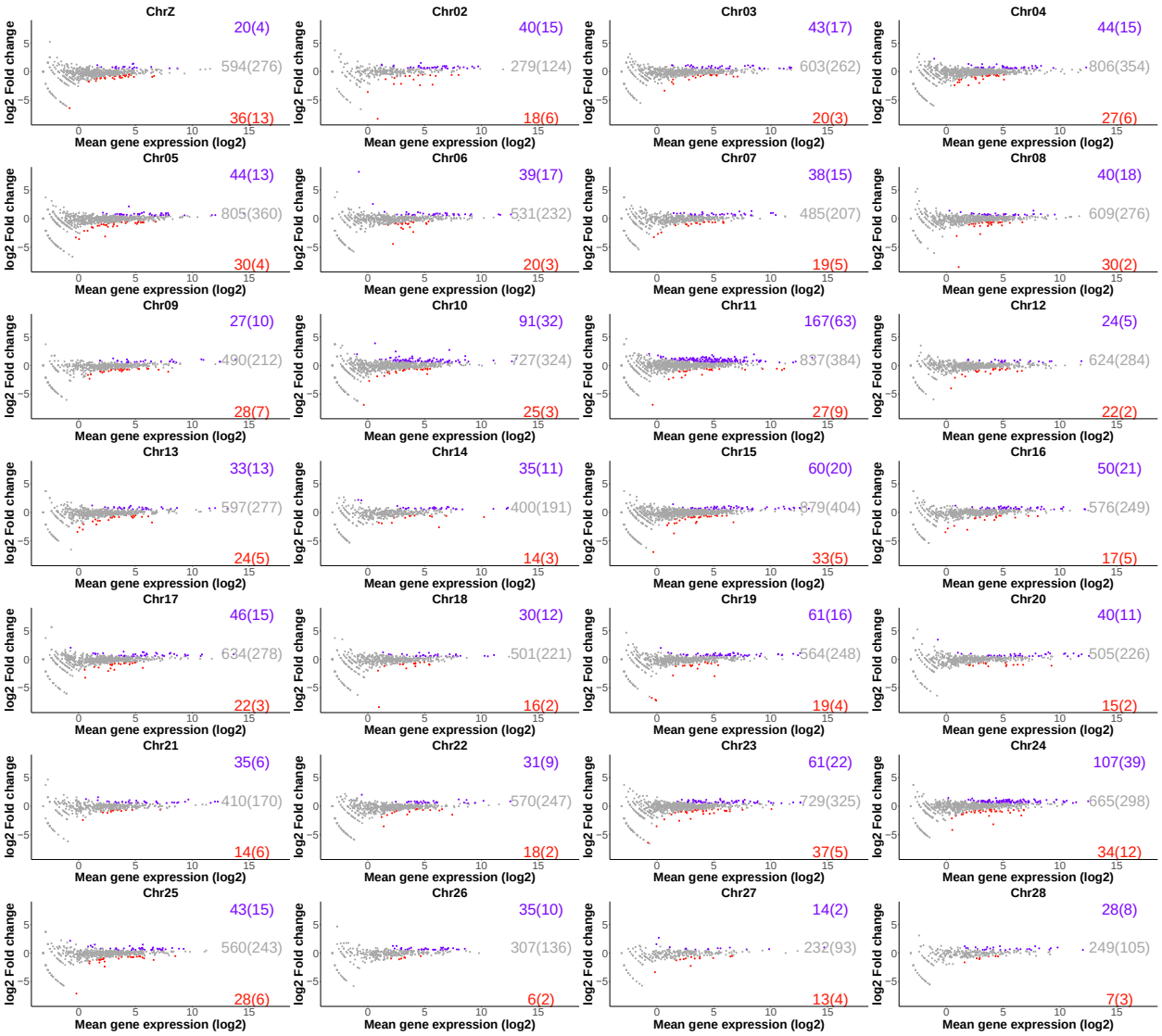

Figure S7. Single chromosome MA plots for mid embryos.

MA plots showing differential expression on all individual chromosomes between male and female mid embryos. Loci with significantly differential expression (FDR < 0.01 and |log2 fold change| > 0.5) are shown in red (male-biased) or purple (female-biased). Total numbers of differential or equally expressed loci are indicated to the right. Numbers inside parentheses indicate intergenic regions.

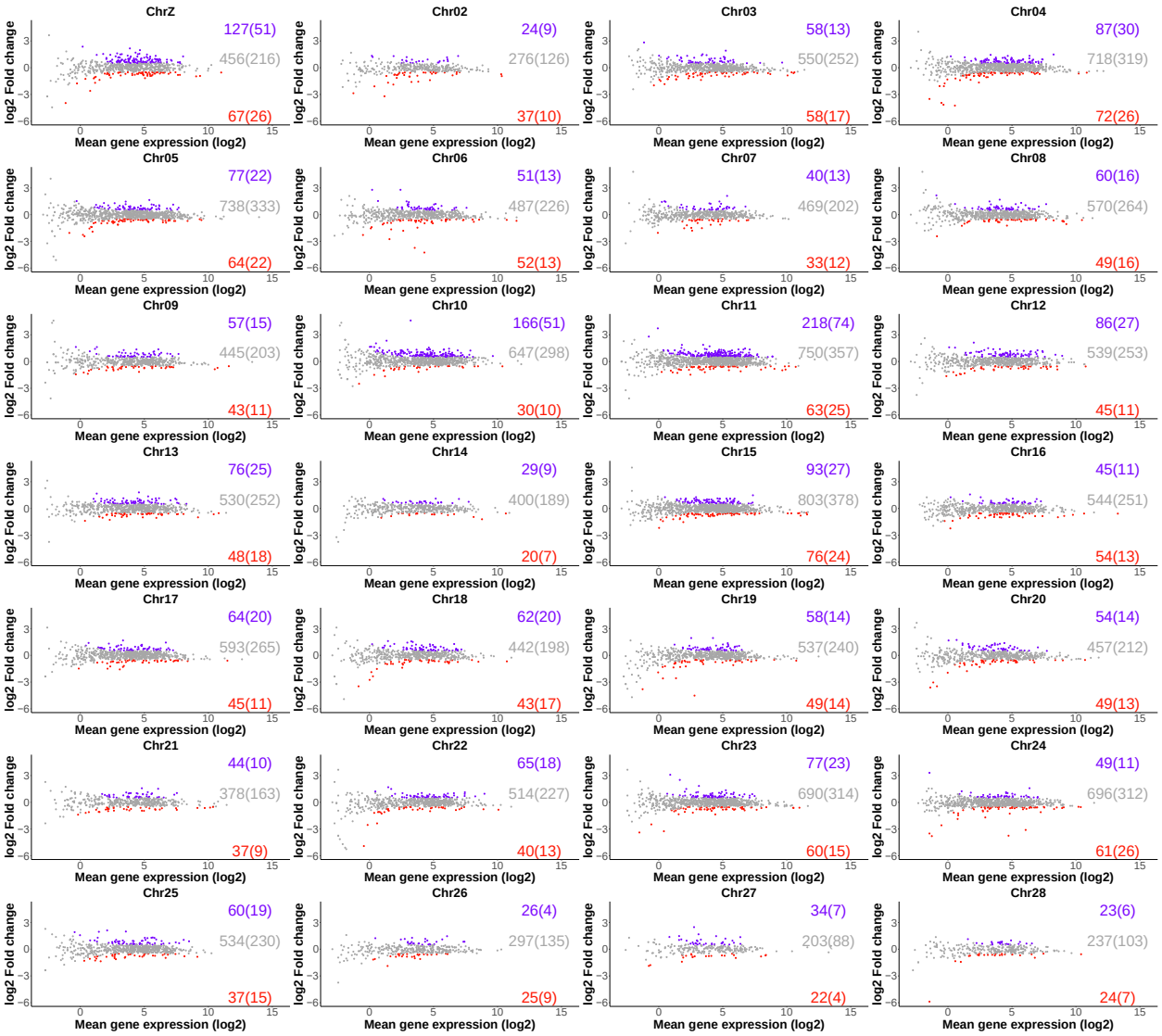

Figure S8. Single chromosome MA plots for late embryos.

MA plots showing differential expression on all individual chromosomes between male and female Late embryos. Loci with significantly differential expression (FDR < 0.01 and |log2 fold change| > 0.5) are shown in red (male-biased) or purple (female-biased). Total numbers of differential or equally expressed loci are indicated to the right. Numbers inside parentheses indicate intergenic regions.

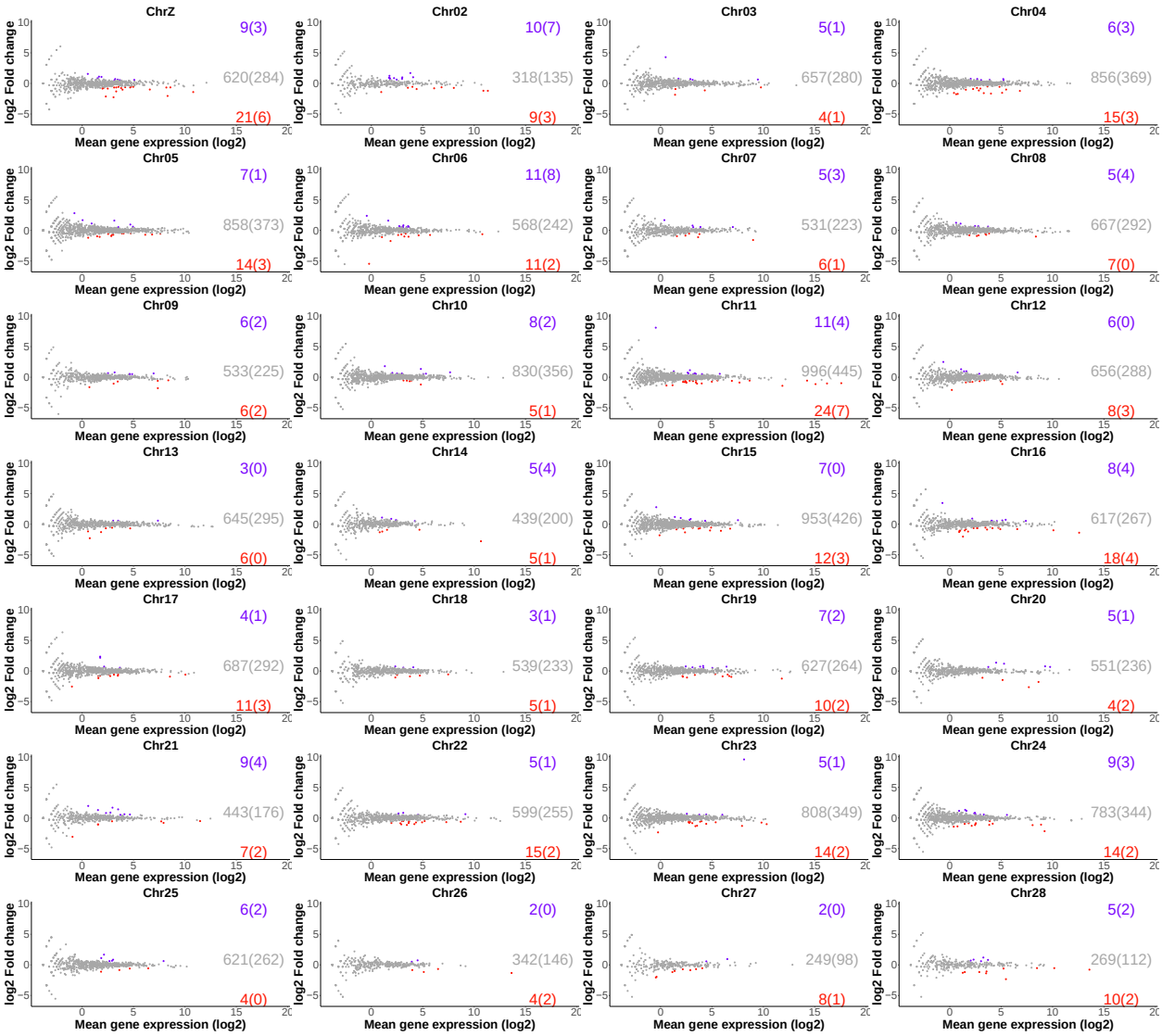

Figure S9. Single chromosome MA plots for larval heads.

MA plots showing differential expression on all individual chromosomes between male and female larval heads. Loci with significantly differential expression (FDR < 0.01 and |log2 fold change| > 0.5) are shown in red (male-biased) or purple (female-biased). Total numbers of differential or equally expressed loci are indicated to the right. Numbers inside parentheses indicate intergenic regions.

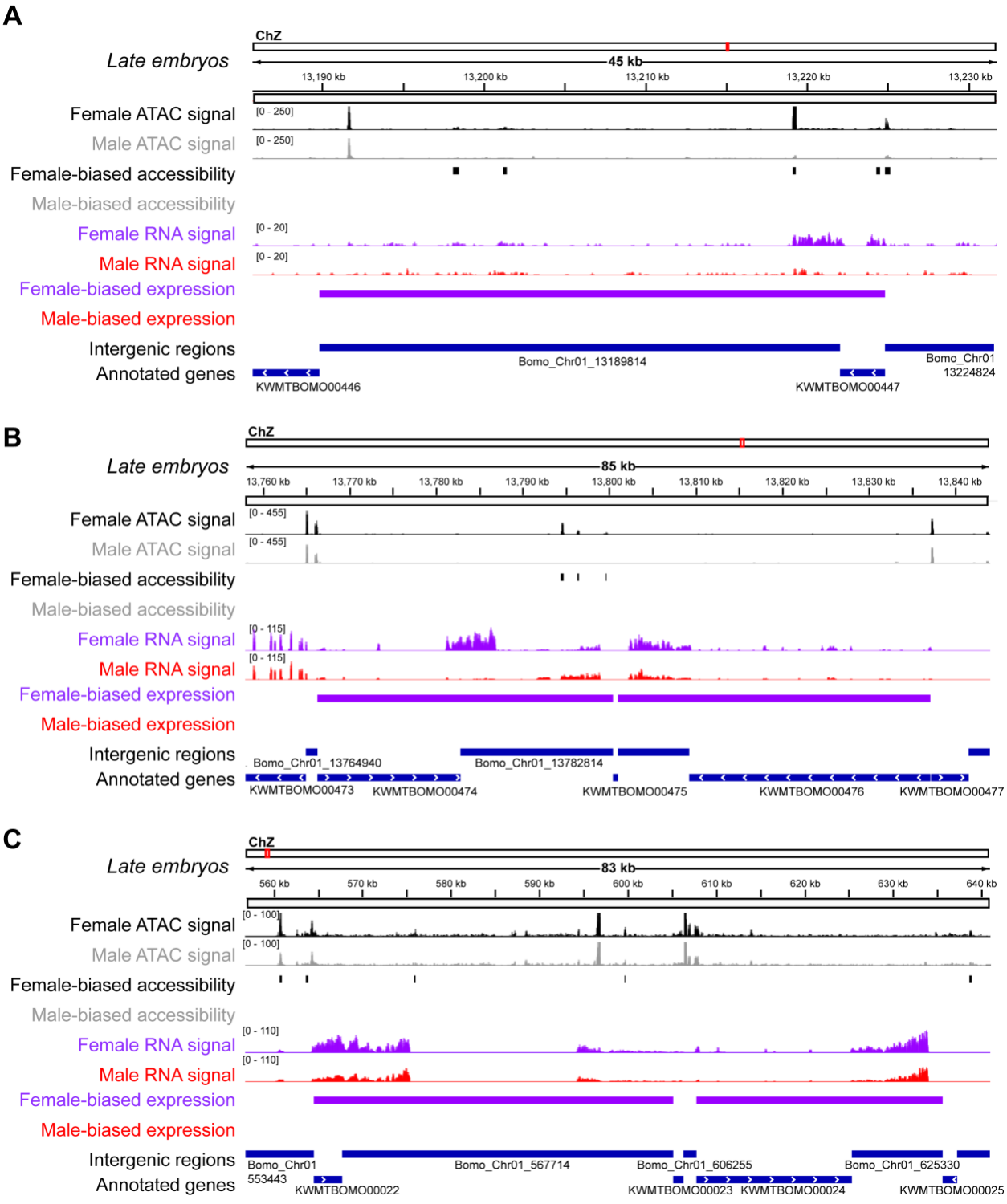
A
Late embryos
ChZ
45 kb
13,190 kb
13,200 kb
13,210 kb
13,220 kb
13,230 kb
Female ATAC signal
[0 - 250]
Male ATAC signal
[0 - 250]
Female-biased accessibility
Male-biased accessibility
Female RNA signal
[0 - 20]
Male RNA signal
[0 - 20]
Female-biased expression
Male-biased expression
Intergenic regions
Annotated genes
Bomo_Chr01_13189814
Bomo_Chr01
13224824
KWMTBOMO00446
KWMTBOMO00447
B
Late embryos
ChZ
85 kb
13,760 kb
13,770 kb
13,780 kb
13,790 kb
13,800 kb
13,810 kb
13,820 kb
13,830 kb
13,840 kb
Female ATAC signal
[0 - 455]
Male ATAC signal
[0 - 455]
Female-biased accessibility
Male-biased accessibility
Female RNA signal
[0 - 115]
Male RNA signal
[0 - 115]
Female-biased expression
Male-biased expression
Intergenic regions
Annotated genes
Bomo_Chr01_13764940
Bomo_Chr01_13782814
KWMTBOMO00473
KWMTBOMO00474
KWMTBOMO00475
KWMTBOMO00476
KWMTBOMO00477
C
Late embryos
ChZ
83 kb
560 kb
570 kb
580 kb
590 kb
600 kb
610 kb
620 kb
630 kb
640 kb
Female ATAC signal
[0 - 100]
Male ATAC signal
[0 - 100]
Female-biased accessibility
Male-biased accessibility
Female RNA signal
[0 - 110]
Male RNA signal
[0 - 110]
Female-biased expression
Male-biased expression
Intergenic regions
Annotated genes
Bomo_Chr01
553443
Bomo_Chr01_567714
Bomo_Chr01_606255
Bomo_Chr01_625330
KWMTBOMO00022
KWMTBOMO00023
KWMTBOMO00024
KWMTBOMO00025

Figure S10. Female-biased accessibility is associated with female-biased expression in late embryos.

A-C. Genome browser screenshots of chZ in late embryos showing ATAC-seq in black and gray (female and male, respectively), RNA-seq in purple and red (female and male, respectively) along with published gene annotations (bottom) and intergenic regions (second from bottom) in blue. Differential ATAC-seq peaks are shown in black (female-biased) and gray (male-biased). Differentially expressed loci are shown in purple (female-biased) and red (male-biased).

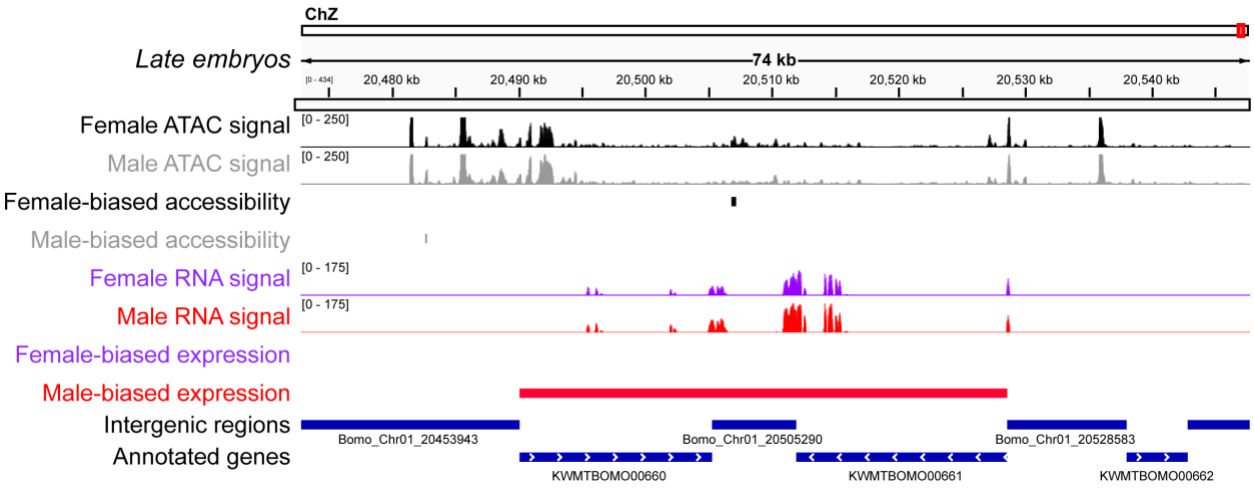

Figure S11. Male-biased accessibility is not associated with male-biased expression in late embryos.

Genome browser screenshot of chZ in late embryos (showing ATAC-seq in black and gray (female and male, respectively), RNA-seq in purple and red (female and male, respectively) along with published gene annotations (bottom) and intergenic regions (second from bottom) in blue. Differential ATAC-seq peaks are shown in black (female-biased) and gray (male-biased). Differentially expressed loci are shown in purple (female-biased) and red (male-biased).

Supplemental Tables

Table S1. Chromosome and chromosome paint information

Chrom.	Chromosome size (bp)	Size painted (bp)	Paint start	Paint stop	Density (probes/kb)	Total # of oligos	Gene density (genes per Mb)
4	18,737,234	18,639,239	282	18,639,521	1.5	26,841	39.71
7	13,944,894	13,868,845	35,931	13,904,776	3	42,625	36.00
15	18,440,292	18,354,755	21,089	18,375,844	1	17,756	43.60
16	14,337,292	14,275,583	27,737	14,303,320	1.5	20,190	43.66
17	16,840,672	16,806,551	9,415	16,815,966	1.5	23,834	38.30
23	21,465,692	21,339,065	123,188	21,462,253	1.5	30,506	35.82
Z (1)	20,666,287	20,578,020	37,936	20,615,956	1.5	29,784	32.18

Table S2. Stripe sub-library paint information

Chrom.	Tel1 size (Mb)	Mid size (Mb)	Tel2 size (Mb)	Density (probes/kb)
7	2.77	2.76	2.77	3
15	3.66	3.68	3.62	1
16	2.84	2.84	2.84	1.5
23	3.16	1.65	3.30	1.5
Z (1)	3.12	1.58	3.06	1.5

Table S3. Differentially expressed Z-linked genes and intergenic regions in late embryos

Female-biased expression	Male-biased expression
Bomo_Chr01_10231768_10251279	Bomo_Chr01_10334568_10353388
Bomo_Chr01_10265998_10266902	Bomo_Chr01_11417998_11423958
Bomo_Chr01_10269488_10281672	Bomo_Chr01_13899609_13903630
Bomo_Chr01_10567168_10573044	Bomo_Chr01_14263038_14264848
Bomo_Chr01_10914049_10925807	Bomo_Chr01_15435166_15435442
Bomo_Chr01_11018177_11030129	Bomo_Chr01_16061069_16069509
Bomo_Chr01_11969591_11977059	Bomo_Chr01_17032456_17076840
Bomo_Chr01_12003226_12071853	Bomo_Chr01_17396912_17408872
Bomo_Chr01_12422168_12433748	Bomo_Chr01_18626741_18678058
Bomo_Chr01_12467587_12478148	Bomo_Chr01_20024276_20026864

Bomo_Chr01_12788526_12879762	Bomo_Chr01_20060295_20064403
Bomo_Chr01_13189814_13222021	Bomo_Chr01_20218200_20269653
Bomo_Chr01_13252844_13259444	Bomo_Chr01_20335893_20345266
Bomo_Chr01_1333887_1334678	Bomo_Chr01_20349319_20379382
Bomo_Chr01_13782814_13800437	Bomo_Chr01_20505290_20511932
Bomo_Chr01_13801014_13809208	Bomo_Chr01_20599483_20666287
Bomo_Chr01_14124359_14143677	Bomo_Chr01_3429803_3557390
Bomo_Chr01_14417060_14425543	Bomo_Chr01_454225_487675
Bomo_Chr01_1469527_1490070	Bomo_Chr01_5713711_5790723
Bomo_Chr01_1510551_1519820	Bomo_Chr01_5958396_5963212
Bomo_Chr01_15417762_15425214	Bomo_Chr01_6147892_6151386
Bomo_Chr01_17356042_17363367	Bomo_Chr01_6446320_6453988
Bomo_Chr01_17415426_17427702	Bomo_Chr01_71352_78817
Bomo_Chr01_1775110_1791901	Bomo_Chr01_7326344_7381173
Bomo_Chr01_19363856_19372571	Bomo_Chr01_8532965_8534205
Bomo_Chr01_19471945_19487619	Bomo_Chr01_9445867_9447037
Bomo_Chr01_1958266_1964535	KWMTBOMO00019
Bomo_Chr01_19766154_19774511	KWMTBOMO00020
Bomo_Chr01_1991877_1996582	KWMTBOMO00111
Bomo_Chr01_1997246_2001181	KWMTBOMO00122
Bomo_Chr01_2307813_2315356	KWMTBOMO00171
Bomo_Chr01_2541009_2555579	KWMTBOMO00184
Bomo_Chr01_3107821_3128546	KWMTBOMO00192
Bomo_Chr01_4360131_4397238	KWMTBOMO00221
Bomo_Chr01_4784783_4794824	KWMTBOMO00243
Bomo_Chr01_4927123_4954325	KWMTBOMO00254
Bomo_Chr01_5047459_5065887	KWMTBOMO00255
Bomo_Chr01_5644852_5651469	KWMTBOMO00262
Bomo_Chr01_567714_605123	KWMTBOMO00270
Bomo_Chr01_6218332_6227133	KWMTBOMO00293
Bomo_Chr01_625330_635578	KWMTBOMO00298
Bomo_Chr01_7490369_7512340	KWMTBOMO00302
Bomo_Chr01_8464105_8474245	KWMTBOMO00332
Bomo_Chr01_8633205_8640243	KWMTBOMO00333
Bomo_Chr01_8779922_8786289	KWMTBOMO00339
Bomo_Chr01_8820845_8843412	KWMTBOMO00380
Bomo_Chr01_8925412_8950822	KWMTBOMO00387
Bomo_Chr01_9432317_9439662	KWMTBOMO00390
Bomo_Chr01_9745824_9756340	KWMTBOMO00391

Bomo_Chr01_9811704_9818805	KWMTBOMO00420
Bomo_Chr01_9959680_9965054	KWMTBOMO00421
KWMTBOMO00022	KWMTBOMO00458
KWMTBOMO00024	KWMTBOMO00479
KWMTBOMO00051	KWMTBOMO00494
KWMTBOMO00057	KWMTBOMO00521
KWMTBOMO00060	KWMTBOMO00530
KWMTBOMO00061	KWMTBOMO00531
KWMTBOMO00064	KWMTBOMO00542
KWMTBOMO00065	KWMTBOMO00543
KWMTBOMO00067	KWMTBOMO00583
KWMTBOMO00068	KWMTBOMO00585
KWMTBOMO00079	KWMTBOMO00592
KWMTBOMO00086	KWMTBOMO00614
KWMTBOMO00104	KWMTBOMO00644
KWMTBOMO00135	KWMTBOMO00650
KWMTBOMO00155	KWMTBOMO00660
KWMTBOMO00157	KWMTBOMO00661
KWMTBOMO00158	
KWMTBOMO00160	
KWMTBOMO00168	
KWMTBOMO00177	
KWMTBOMO00178	
KWMTBOMO00179	
KWMTBOMO00181	
KWMTBOMO00186	
KWMTBOMO00190	
KWMTBOMO00240	
KWMTBOMO00242	
KWMTBOMO00249	
KWMTBOMO00264	
KWMTBOMO00273	
KWMTBOMO00274	
KWMTBOMO00281	
KWMTBOMO00290	
KWMTBOMO00300	
KWMTBOMO00301	
KWMTBOMO00303	
KWMTBOMO00306	

KWMTBOMO00308	
KWMTBOMO00314	
KWMTBOMO00319	
KWMTBOMO00321	
KWMTBOMO00327	
KWMTBOMO00328	
KWMTBOMO00331	
KWMTBOMO00336	
KWMTBOMO00337	
KWMTBOMO00352	
KWMTBOMO00353	
KWMTBOMO00363	
KWMTBOMO00364	
KWMTBOMO00366	
KWMTBOMO00382	
KWMTBOMO00407	
KWMTBOMO00411	
KWMTBOMO00425	
KWMTBOMO00426	
KWMTBOMO00435	
KWMTBOMO00447	
KWMTBOMO00455	
KWMTBOMO00460	
KWMTBOMO00465	
KWMTBOMO00474	
KWMTBOMO00476	
KWMTBOMO00495	
KWMTBOMO00507	
KWMTBOMO00535	
KWMTBOMO00537	
KWMTBOMO00539	
KWMTBOMO00557	
KWMTBOMO00582	
KWMTBOMO00588	
KWMTBOMO00621	
KWMTBOMO00623	
KWMTBOMO00633	
KWMTBOMO00639	
KWMTBOMO00640	

Table S4. Differentially expressed Z-linked genes and intergenic regions in larval heads

Female-biased expression	Male-biased expression
Bomo_Chr01_13439491_13448180	Bomo_Chr01_18626741_18678058
KWMTBOMO00501	KWMTBOMO00530
KWMTBOMO00650	Bomo_Chr01_18678943_18727908
Bomo_Chr01_15773905_15796285	KWMTBOMO00339
KWMTBOMO00222	KWMTBOMO00390
KWMTBOMO00435	Bomo_Chr01_8307450_8385610
KWMTBOMO00021	KWMTBOMO00422
Bomo_Chr01_13782814_13800437	Bomo_Chr01_71352_78817
KWMTBOMO00474	Bomo_Chr01_8423403_8428229
	KWMTBOMO00661
	KWMTBOMO00086
	KWMTBOMO00224
	KWMTBOMO00610
	KWMTBOMO00496
	KWMTBOMO00211
	KWMTBOMO00543
	KWMTBOMO00592
	KWMTBOMO00391
	KWMTBOMO00382
	KWMTBOMO00091
	Bomo_Chr01_545938_548702

Extended Methods

B. mori embryonic and larval cell slide preparation

Mid and late embryos were partially dechorionated in 50% bleach for 15 min at RT, followed by manual removal of the chorion and vitelline membrane with forceps in a glass dissecting dish containing RT Sf-900 media (Gibco). For mid embryos, cells were then harvested directly from the dissecting dish and settled on poly-L-lysine-treated glass slides for 30 min in media before fixing with 4% PFA in PBS. For late embryos, pre-larvae were manually dissected away from extra-embryonic tissue and cells were dissociated with papain and collagenase before settling on slides and fixing as above. For larval samples, heads from 5th instar larvae were collected by decapitation, and cells were dissociated using Papain and Collagenase. Single embryos or single larval heads were used for slides involving Z chromosome analyses, and the number of Z chromosomes was used to sex the embryos. Larvae were sexed during dissection based on gonad morphology.

Nuclear volume analyses across species

L4 *C. elegans* (Bristol N2) were aged 24 h before harvesting. Whole worms were prepared and DAPI stained as previously described (1). Briefly, worms were fixed in 8% PFA in PBS for 1 h at RT, washed with PBS, permeabilized with 95% ethanol for 1 min, and then stained with DAPI.

Mouse p1 eyes were prepared as previously described (2). Briefly, eyes were dissected from p1 mice and fixed in 4% PFA in PBS for up to 4 h. Eyes were then soaked in 15% sucrose for 1-2 d (until the tissue sinks in solution). This was repeated with 30% sucrose. Eyes were then

immersed in OCT Tissue Freezing Medium (Leica) and frozen on dry ice. Slides were prepared by cryosectioning into 16 µm slices using a Cryostat (Leica). Tissue slides were then fixed again with 4% PFA for 15 min before staining with DAPI and mounting with Prolong Diamond.

Dictyostelium (*D. discoideum*) were removed from their culture medium by centrifugation at 600 x*g* for 5 min, then resuspended in PBS. Cells were settled onto Poly-L lysine coated slides for 10 min before fixing for 15 min with 4% PFA in PBS. Slides were washed thrice with PBS and before DAPI staining and mounting.

For all species, including *Drosophila* and *Bombyx*, nuclear diameters were manually measured in ImageJ, and nuclear volumes were then calculated in Microsoft Excel.

Oligopaint multiplexing

Whole chromosome paints were multiplexed as previously described (3, 4) to allow for amplification sub-chromosomal stripes. Chromosomes 7, 15, and 16 contain 5 sub-chromosomal stripes approximately 3 Mb each. Of these, stripes 1, 3, and 5 were labeled to generate the 3-stripe pattern (tel1, mid, and tel2, respectively). Chromosomes Z and 23 contain 13 sub-chromosomal stripes approximately 1.5 Mb each. For chZ and ch23, stripes 1,2 (combined = tel1), 7 (mid), and 12, 13 (combined = tel2) were labeled to generate the 3-stripe pattern.

Oligopaint DNA FISH in *B. mori* cells

After slide preparation and fixation as described above, slides were washed 3x 5 min each in 0.1% Triton X-100 in PBS (PBS-$T^{0.1\%}$) at RT, then permeabilized with PBS-$T^{0.5\%}$ for 15 min

at RT. Cells were subsequently pre-denatured using the following washes: 1x 5 min in 2xSSCT (0.3 M NaCl, 0.03 M sodium citrate, 0.1% Tween-20) at RT, 1x 5 min 2xSSCT/50% formamide at RT, 1x 2.5 min in 2×SSCT/50% formamide at 92°C, 1x 20 min at 60°C in 2xSSCT/50% formamide. Primary Oligopaint probes in hybridization buffer (10% dextran sulfate/2xSSCT/50% formamide/4% polyvinylsulfonic acid) were then added to slides, covered with 22x22 mm cover glass, and sealed before being denatured at 92°C for 2.5 min. Slides were then placed in a humidified chamber at 37°C and incubated 16-18 h. The next day, slides were washed as follows: 2xSSCT at 60°C for 15 min, 2xSSCT at RT for 15 min, 0.2xSSC at RT for 10 min. Secondary probes (10 pmol/25 µL) containing fluorophores were added to slides, resuspended in hybridization buffer as described above, and covered with 22x22 mm cover glass and sealed. Slides were incubated at 37°C in a humidified chamber for 2 h before repeating the above washes. Finally, all slides were stained with DAPI DNA stain in PBS for 5 min, followed by 2x 5 min washes in PBS- $T^{0.1\%}$ before mounting in Prolong Diamond (Invitrogen). Slides were left to cure overnight at RT before sealing with nail polish.

RNA-seq analysis

Raw RNA-seq data were downloaded from BioProjectID: PRJNA388026. Adaptors were detected by BBtools v38.82 (5). Low quality bases and adaptors were trimmed using trimgalore v0.6.5 (6). The filtered paired-end reads were mapped to an updated version of the Ensembl (2013) *Bombyx mori* (ASM15162v1) reference genome using bowtie v2.4.1 (7) with default parameters in paired-end mode. SAM/BAM conversions, sorting, indexing and filtering were performed with SAMtools v. 1.10 (8). Aligned reads in the bam files were counted using

subread featureCounts v2.0.1 (9) with default parameters. The GTF file was downloaded from Silkbase (2016 gene models). In addition to annotated genes, intergenic regions were analyzed to circumvent problems with annotation. Raw read counts were normalized by fpkm (Fragments Per Kilobase of transcript per Million mapped reads). All annotated genes were grouped into autosomal (A)- or Z-linked (Z) genes. Genes that were not expressed in any samples (raw fpkm < 0.01 in all samples) were removed from analyses. After filtering, the total gene number was 17,713. Significant female- or male-biased expression was defined as FDR < 0.01 and |log2 fold change| > 0.5 using edgeR (10). For direct comparisons of chZ to autosomes (such as Figure 6D-E), all genes with fpkm < 0.01 were removed from individual samples, leaving only the expressed genes present in each data set. Median fpkm values of genes on Z and autosomes were used to compute Z:A ratios. Z-linked genes and intergenes with significantly sex-biased expression can be found in Tables S3 and S4.

ATAC-seq sample preparation and data analysis

ATAC-seq was performed using the ATAC-seq Kit from Active Motif (cat#53150) according to the manufacturer's instructions. For embryos, 16 single embryos were isolated and dissociated as described above. Then 10 µL of cells were harvested, fixed to slides, and subjected to DNA FISH with chZ paint. Embryos were sexed based on the number of chZ foci present on slides, and the remaining cells were used to generate ATAC-seq libraries. Tn5-tagmented chromatin from two male or two female embryos was then pooled for library preparation, creating a total of 3 male and 3 female biological replicates (two embryos per library replicate). For larvae, heads were harvested by dissection, and larvae were sexed based

on internal gonad morphology. ATAC-seq libraries were generated with individual larval samples (one larva per replicate). Libraries were double size-selected with AMPure XP beads (Beckman Coulter; 0.6× volume followed by 1.2× volume).

ATAC-seq libraries were sequenced using the NovaSeq 6000 SP, PE 150bp with 300 cycles (Illumina) at the NHLBI Sequencing and Genomics core and analyzed as previously described (11). Sequencing reads were trimmed for adapters with cutadapt (v2.3) and aligned to an updated version of the Ensembl (2013) *Bombyx mori* (ASM15162v1) reference genome with bowtie2 (v2.3.5; --very-sensitive, paired-end mode; (7)). For proper normalization, reads from ch Z and autosomes were analyzed separately. Reads were depleted of multi-mapped reads with samtools (v1.9; (8)) and PCR duplicates with picard (MarkDuplicates REMOVE_DUPLICATES=true) were further selected for inserts < 150 bp to perform peak calling with MACS2 (v2.2.6; pair-end mode -f BAMPE; (12)). Differential accessibility was called with the R package DiffBind v2.6.6 ((13); edgeR, $p<0.05$) and associated with the closest gene to generate MA plots integrating RNA-seq data. The *p* values of Fisher's exact tests were calculated for expressed genes (fpkm > 0.01) with R v3.6.1 and reported as two-tailed values with ***$p < 0.001$, **$p < 0.01$ and *$p < 0.05$. Heatmaps were generated with deepTools (v3.5.1; (14)). The ATAC-seq data have been deposited in the Gene Expression Omnibus database under accession number GSE191164.

Supplemental References

1. S. Shaham, *Methods in cell biology* (WormBook, 2006) (December 2, 2021).

2. H. Léger, E. Santana, W. A. Beltran, F. C. Luca, Preparation of Mouse Retinal Cryo-sections for Immunohistochemistry. *J Vis Exp* (2019) https:/doi.org/10.3791/59683.

3. B. D. Fields, S. C. Nguyen, G. Nir, S. Kennedy, A multiplexed DNA FISH strategy for assessing genome architecture in Caenorhabditis elegans. *eLife* **8** (2019).

4. L. F. Rosin, J. G. Jr, I. A. Drinnenberg, E. P. Lei, Oligopaint DNA FISH reveals telomere-based meiotic pairing dynamics in the silkworm, Bombyx mori. *PLOS Genetics* **17**, e1009700 (2021).

5. B. Bushnell, J. Rood, E. Singer, BBMerge - Accurate paired shotgun read merging via overlap. *PLoS One* **12**, e0185056 (2017).

6. F. Krueger, F. James, P. Ewels, E. Afyounian, B. Schuster-Boeckler, *FelixKrueger/TrimGalore: v0.6.7 - DOI via Zenodo* (Zenodo, 2021) https:/doi.org/10.5281/zenodo.5127899 (December 12, 2021).

7. B. Langmead, S. Salzberg, Fast gapped-read alignment with Bowtie 2 | Nature Methods. *Nature Methods* (2012) https:/doi.org/10.1038/nmeth.1923 (April 19, 2021).

8. H. Li, *et al.*, The Sequence Alignment/Map format and SAMtools. *Bioinformatics* **25**, 2078–2079 (2009).

9. Y. Liao, G. K. Smyth, W. Shi, featureCounts: an efficient general purpose program for assigning sequence reads to genomic features. *Bioinformatics* **30**, 923–930 (2014).

10. M. D. Robinson, D. J. McCarthy, G. K. Smyth, edgeR: a Bioconductor package for differential expression analysis of digital gene expression data. *Bioinformatics* **26**, 139–140 (2010).

11. D. Chen, C. E. McManus, B. Radmanesh, L. H. Matzat, E. P. Lei, Temporal inhibition of chromatin looping and enhancer accessibility during neuronal remodeling. *Nat Commun* **12**, 6366 (2021).

12. Y. Zhang, *et al.*, Model-based Analysis of ChIP-Seq (MACS). *Genome Biology* **9**, R137 (2008).

13. R. Stark, G. Brown, DiffBind: Differential binding analysis of ChIP-Seq peak data. 75.

14. F. Ramírez, F. Dündar, S. Diehl, B. A. Grüning, T. Manke, deepTools: a flexible platform for exploring deep-sequencing data. *Nucleic Acids Res* **42**, W187-191 (2014).